

Study of cadmium-induced cytotoxicity using two-photon excitation endogenous fluorescence microscopy

Dong Li

Hong Kong University of Science and Technology
Department of Electronic and Computer Engineering
Clear Water Bay
Kowloon, Hong Kong
China

Mildred S. Yang[†]

Tao Lin^{*}

Hong Kong Baptist University
Department of Biology
Kowloon, Hong Kong
China

Wei Zheng

Jianan Y. Qu[‡]

Hong Kong University of Science and Technology
Department of Electronic and Computer Engineering
Clear Water Bay
Kowloon, Hong Kong
China

Abstract. We demonstrate that using time-resolved two-photon excitation endogenous fluorescence microscopy, the cadmium (Cd)-induced cellular toxic level can be assessed by the free-to protein-bound reduced nicotinamide adenine dinucleotide (free/bound NADH) ratio in a living cell. NADH fluorescence excited at 730 nm is captured at different times following exposure to cadmium at a variety of concentrations. The temporal characteristics of NADH fluorescence from mitochondrial and nuclear compartments are analyzed, respectively. The results show that cadmium induces a significant increase of the free/bound NADH ratio in mitochondria and nucleus, caused by the inhibition effect on the electron transport chain (ETC) and the stimulating effect on the glycolysis pathway, respectively. It is found that induction of metallothionein (MT) in cells occurs after 4 h of exposure to a sublethal concentration of Cd and reaches a peak at 6 h. More importantly, the increase in MT level can effectively suppress the elevation of the free/bound NADH ratio caused by a subsequent exposure to a higher concentration of Cd, indicating that MT plays a key role in protecting cells from Cd-induced toxicity. Our findings show that the free/bound NADH ratio can potentially be used as a sensitive indicator of toxic and carcinogenic actions induced by Cd. © 2009 Society of Photo-Optical Instrumentation Engineers. [DOI: 10.1117/1.3250293]

Keywords: multiphoton microscopy; time-resolved fluorescence; metabolism; cadmium toxicity; metallothionein.

Paper 09073RR received Mar. 5, 2009; revised manuscript received Aug. 6, 2009; accepted for publication Aug. 11, 2009; published online Oct. 23, 2009.

1 Introduction

Heavy metals are toxic industrial and environmental pollutants associated with many industrial processes. Their toxicity can result in DNA damage that causes an increased risk of cancer and damage to the nervous system and vital organs such as the lung, kidney, and liver.^{1,2} Cadmium (Cd) is a representative heavy metal whose toxic effects are similar to those of other heavy metals, such as lead, mercury, and arsenic.^{2,3} In the United States, it has been estimated that each year approximately 512,000 workers are in environments where Cd exposure may occur.⁴ The cellular responses to Cd exposure are complicated. For instance, Cd can interfere with cellular metabolic processes, the intracellular signaling network, and gene regulation.⁵ At a high concentration, Cd can cause cell death via apoptosis.⁶ In contrast, cells tend to tol-

erate a low Cd concentration, mainly due to the induction of the antioxidant protein metallothionein¹ (MT). The state of the art for measuring toxic effects in cells or tissues employs many biochemical methods with complicated procedures, usually under invasive and *ex vivo* condition.⁵⁻¹¹ It is desirable to monitor and evaluate the toxic level in living cells and tissues noninvasively and continuously when studying the mechanism of heavy metal toxicity and developing antitoxic or therapeutic drugs.^{8,9} We demonstrate that time-resolved two-photon excitation endogenous fluorescence (TPEF) microscopy could perform noninvasive time-lapse measurement of Cd-induced toxic effects in living biological system. This method could be potentially used for noninvasive monitoring of toxicity in living biological system induced by other heavy metals that produce toxic effects similar to those from Cd.

Previous studies demonstrated that Cd could affect the function of certain enzymes that are involved in energy metabolism.^{5,11} It is known that reduced nicotinamide adenine dinucleotide (NADH) is a metabolic coenzyme playing important roles in a variety of cellular metabolic pathways. In mitochondria, NADH is the major electron donor of the electron transport chain. In cytosol, NAD⁺ and NADH mediate

^{*}Current address: Department of Environmental Toxicology, University of Washington, Seattle, Washington.

[†]Address correspondence for toxicology to: Mildred S. Yang, Doctor, Department of Biology, Hong Kong Baptist University, Kowloon, Hong Kong. Tel: 852-3411-7058; Fax: 852-3411-5995; E-mail: msyang@hkbu.edu.hk

[‡]Address correspondence for fluorescence microscopy to: Jianan Y. Qu, Doctor, Department of Electronic and Computer Engineering, Hong Kong University of Science and Technology, Clear Water Bay, Kowloon, Hong Kong. Tel: 852-2358-8541; Fax: 852-2358-1485; E-mail: eequ@ust.hk

glycolysis via the oxidation of glyceraldehydes 3-phosphate to 1,3-bisphosphoglycerate and the lactate-pyruvate conversions catalyzed by lactate dehydrogenase. NADH functions in these biological processes by binding to many enzymes.¹² A recent study showed that Cd can inhibit the activity in yeast of glutathione reductase, which is a kind of enzyme that NADH binds to.¹³ Moreover, the free/bound NADH ratio has been employed as a sensitive indicator for cellular metabolic status in many studies.^{14–17} Therefore, it is suggested that the free/bound NADH ratio could serve as a sensitive indicator of the toxic level associated with Cd-induced changes of cellular metabolism and enzyme activity. In this study, time-resolved TPEF microscopy is used to characterize a change of the free/bound NADH ratio in living cell samples during exposure to lethal and sublethal concentrations of Cd. By employing the previously developed image segmentation method,¹⁷ the free/bound NADH fluorescence ratios in mitochondrial and nuclear compartments, respectively, were analyzed. We investigated the correlation of the free/bound NADH ratio to Cd-induced toxicity. In particular, our study intends to reveal how the free/bound NADH ratio reflects the important phenomenon that cells pretreated with a sublethal concentration of Cd produce adaptive tolerance to the toxicity induced by subsequent exposure to a much higher dose of Cd. This is important for the development of antitoxic and therapeutic drugs. The results demonstrate that cellular NADH signals could be potentially used to noninvasively monitor Cd-induced cytotoxicity.

2 Methods and Materials

2.1 Samples and Chemicals

The HepG2 cell line (human hepatocellular carcinoma cell line) was purchased from American Type Culture Collection. Minimum essential medium (MEM), fetal bovine serum (FBS), and fungizone were obtained from Invitrogen Corp. (Scotland, United Kingdom). The antibiotics (amphotericin B and penicillin-streptomycin) and phosphate buffered saline (PBS) were from Life Technologies (Gibco, Grand Island, New York). All other chemicals used in this study were of analytical grade and were purchased from Sigma Chemical Co. (St. Louis, Missouri). The HepG2 cells were cultured on a coverslip (Marienfeld Laboratory Glassware, Germany) that was placed in a 35-mm petri dish (Iwaki, Japan) and covered with 1-ml MEM supplemented with 10% FBS, 0.5% antibiotics, and 0.5% fungizone in a humidified atmosphere of 95% air and 5% CO₂.

2.2 Cell Treatment and Viability Study

CdCl₂ (Cd) was made into a stock solution by dissolving the chloride salt in double-distilled water (Millipore) and diluted to the required concentrations. The molarity of Cd was calculated based on a molecular weight of 183.4. Cells were cultured in 24-well plates until confluence was achieved. In the study of Cd-induced cytotoxicity, the medium of each sample was replaced by one containing certain concentration of Cd and the treatment lasted over a period of time of interest. To measure the cell viability after a 24-h treatment, the number of viable cells was determined by the color change of 3-(4,5-dimethylthiazol-2-yl)-2,5-diphenyltetrazolium bromide

(MTT) assay, as described in a previous publication.¹⁸ The viability was calculated based on the percentage of surviving cells over the cells before the treatment.

2.3 Quantification of Cellular MT

MT in the HepG2 cells was measured using a modified method of Cd-binding assay, as described previously.^{10,19} Briefly, at 0, 4, 6, 8, and 24 h after cells were exposed to a sublethal concentration of Cd (5 μM), the medium was removed and cells were trypsinized and collected in an Eppendorf tube. After washing and removing the medium, 1 ml of 0.02 M Tris-HCl buffer, pH 7.4, containing 1 mM PMSF was added. The mixture was lysed by sonication. An aliquot of the lysate was removed for determining total protein content by the method of Bradford (Bio-Rad, U.S.A). The level of protein was calculated from a standard curve constructed simultaneously using BSA as a reference standard. The remaining lysate was centrifuged (5 min at 9000 rpm) and the supernatant was removed, boiled twice at 85 °C for 5 min. The precipitated heat labile protein was removed by centrifugation (5 min, 9000 rpm). To 200 μl of the supernatant, Cd was added to a final concentration of 2 μg/ml. After mixing thoroughly, 100 μl of 2% bovine hemoglobin solution (Type II, Sigma Chemical Co, St. Louis, Missouri) was added. The solution was heated at 100 °C for 2 min and cooled rapidly. This procedure was repeated again. The precipitated hemoglobin to which free Cd was bound, was removed by centrifugation (5 min, 9000 rpm). The MT-bound Cd in the supernatant was measured by graphite furnace atomic absorption spectrometry at a wavelength of 228.8 nm. All solutions were made with double-distilled water (Millipore). Plasticwares were used whenever possible. All glassware and plasticwares were soaked in 5% nitric acid overnight to avoid contamination. MT content was calculated based on the equation described previously¹⁹ and assuming that the molecular weight of MT is 7000 and each mole of MT binds to 7 moles of Cd.

2.4 Imaging Instrumentation

The time-resolved TPEF microscope employs a femtosecond Ti:sapphire laser (Mira 900, Coherent) tuned at 730 nm as the excitation source. A water immersion objective lens [60×, 1.2 numerical aperture (NA), Olympus] was used to focus the excitation beam into the sample and collect the backscattered fluorescence signals. The scanning depth was controlled by an actuator (Model Z625B, Thorlabs). A pair of galvo mirrors scanned the beam laterally and created a 60×60-μm sampling area in the examined sample. The TPEF signal was separated from the excitation light by a dichroic mirror of cutoff wavelength at 650 nm (650DCSX, Chroma) and a shortpass filter of cut-on wavelength at 700 nm (ET700, Chroma). A tube lens with a 80-mm focal length and a 400-μm core optical fiber were used to effectively collect the TPEF signals and conduct the signals to the spectrograph (Model 77400, Oriel). The spectrograph was equipped with a multichannel photomultiplier tube (PMT) and a time-correlated single-photon counting (TCSPC) module (PML-16 and SPC-150, Becker & Hickl GmbH) to measure the time-resolved and spectrally resolved TPEF signals from 400 to 600 nm with an about 13-nm resolution. An electronic

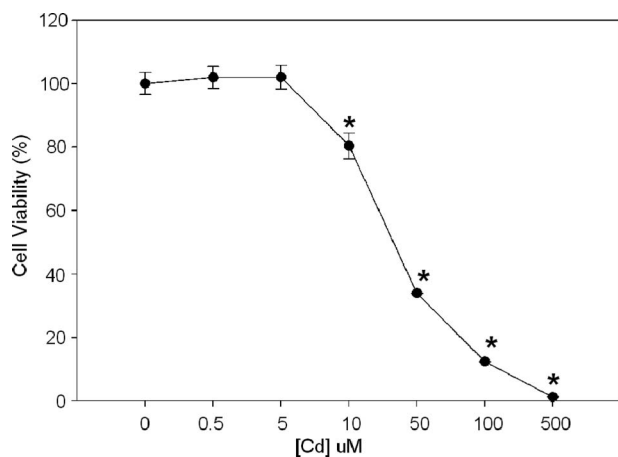


Fig. 1 Viability of cells exposed to different concentrations of Cd for 24 h. Each value represents the mean and standard deviation of 8 replicates. The asterisk indicate that the value is significantly different from that in the control state (maximal $p < 0.01$).

module (PCI-6070E, National Instruments) was used to control the movement of the scanning mirrors and generate the synchronized signals for the TCSPC module.

In this study, three dishes of HepG2 cells were used at each measurement time and four TPEF images were collected from each dish. The minimum spacing between four imaging locations was greater than 500 μm . Each image consists of 128×128 pixels with 256 time channels. The excitation power was about 6 mW on the sample. The exposure time of each image was set to 64 s. The signal quality of each pixel in the image was not sufficiently high to obtain reliable temporal and spectral characteristics of the fluorescence signal. Therefore, we divided the image of a cell into mitochondria and nucleus compartments. The signals of pixels coming from the same compartment in each image were summed into high-quality summed signals, which were used in the analyses of the fluorescence spectra and lifetimes.¹⁷ The fluorescence decay curve was investigated using software (SPCImage, Becker & Hickel GmbH) with an incomplete decay dual-exponential function model, $A_1 \exp(-t/\tau_1) + A_2 \exp(-t/\tau_2) + A_1 \exp[-(t+\Delta\tau)/\tau_1] + A_2 \exp[-(t+\Delta\tau)/\tau_2]$, where τ_1 and τ_2 are the time decay constants (τ_1 is the short-lifetime component and τ_2 is the long-lifetime component) and A_1 and A_2 are the amplitudes of two decay terms, respectively. The lifetime detecting range of the TCSPC module for each excitation pulse $\Delta\tau$ is 12.5 ns. This is determined by the 80-MHz repetition rate of the femtosecond laser. Note that HepG2 cells grow in clusters, so it is difficult to isolate the cytosol compartment accurately. We did not analyze the signal of the cytosol compartment in this study.

3 Results and Discussions

The viability of cells exposed to different concentrations of Cd over 24 h is shown in Fig. 1. As we can see in the figure, a significant decrease of cell viability, indicating cell apoptosis, occurred when the Cd concentration was over 5 μM . The Wilcoxon test was used to compare the viability of cells treated with different concentrations of Cd with that under control conditions. It was found that the cell viability de-

creased significantly after exposed to Cd with a concentration over 10 μM (p value < 0.01 at a 10- μM Cd concentration). However, the change of viability was not statistically significant when the Cd concentration was lower than 5 μM (p value > 0.6). Therefore, we defined 5 μM as the sublethal concentration of Cd. The measurements of NADH fluorescence showed that the free/bound NADH ratio increased monotonically as a function of time when the Cd concentration was over the sublethal concentration. This is consistent with the results of a previous study.²⁰ In this study, we focused on the response of cellular NADH fluorescence signals to the treatment of Cd at a sublethal concentration. Then we investigated how the cells pretreated with a sublethal concentration of Cd responded to subsequent exposure to a much higher concentration of Cd.

To correlate the endogenous fluorescence signals with the Cd-induced toxic status, fluorescence intensity and lifetime images of HepG2 cell samples were measured sequentially after 0, 0.5, 1, 2, 4, 6, 12, and 24 h of treatment with 5 μM Cd. The representative intensity images of NADH fluorescence recorded at different treatment times are shown in Figs. 2(a)–2(h). As we can see, a nucleus with a relatively lower fluorescence intensity appeared as a dark circle. The bright strips and spots around the nucleus were the mitochondria in which NADH mainly concentrated. This was verified by colocalizing the bright strips and spots with rhodamine-123-stained fluorescence patterns of the mitochondria. It was found that there were almost no obvious alterations in cell morphology after the treatment with the sublethal concentration of Cd. However, a significant elevation of fluorescence intensity, especially in the nuclear region, was observed after the treatment, indicating that the cellular responses of the Cd-induced toxic effect accompany the change of cellular endogenous fluorescence signal. To verify that the increased fluorescence was contributed by the NADH signal, we examined the fluorescence spectra of mitochondrial and nuclear compartments after the treatment. The spectra from both compartments displayed typical spectral characteristics of NADH fluorescence with peaks located at 450 nm.^{15,21} This caused us to conclude that the increases of fluorescence intensity were contributed from the increased cellular NADH signal. In principle, under well-controlled conditions the fluorescence intensity could provide information to quantify a change of the oxidation-reduction state in cells.²² However, our homemade two-photon imaging system could not guarantee the negligible day-to-day variation of the measurement conditions, such as optical alignment, excitation power, and optical sectioning depth. Therefore, the fluorescence intensity was not used as quantitative indicator in this study.

NADH is an important electron carrier for a variety of enzymatic reactions where it functions through binding to many enzymes. Thus, a change in free/bound NADH ratio may reflect the activity of these enzymes, which are affected by the Cd toxic effect.¹³ Previous studies demonstrated that a time-resolved fluorescence measurement could readily extract the free and bound NADH and provide reliable and quantitative information in the assessment of biological processes in living cells and tissue.^{14–17} Therefore, in this study, the free/bound NADH ratio extracted from the time decay of the NADH fluorescence was employed for the quantitative sens-

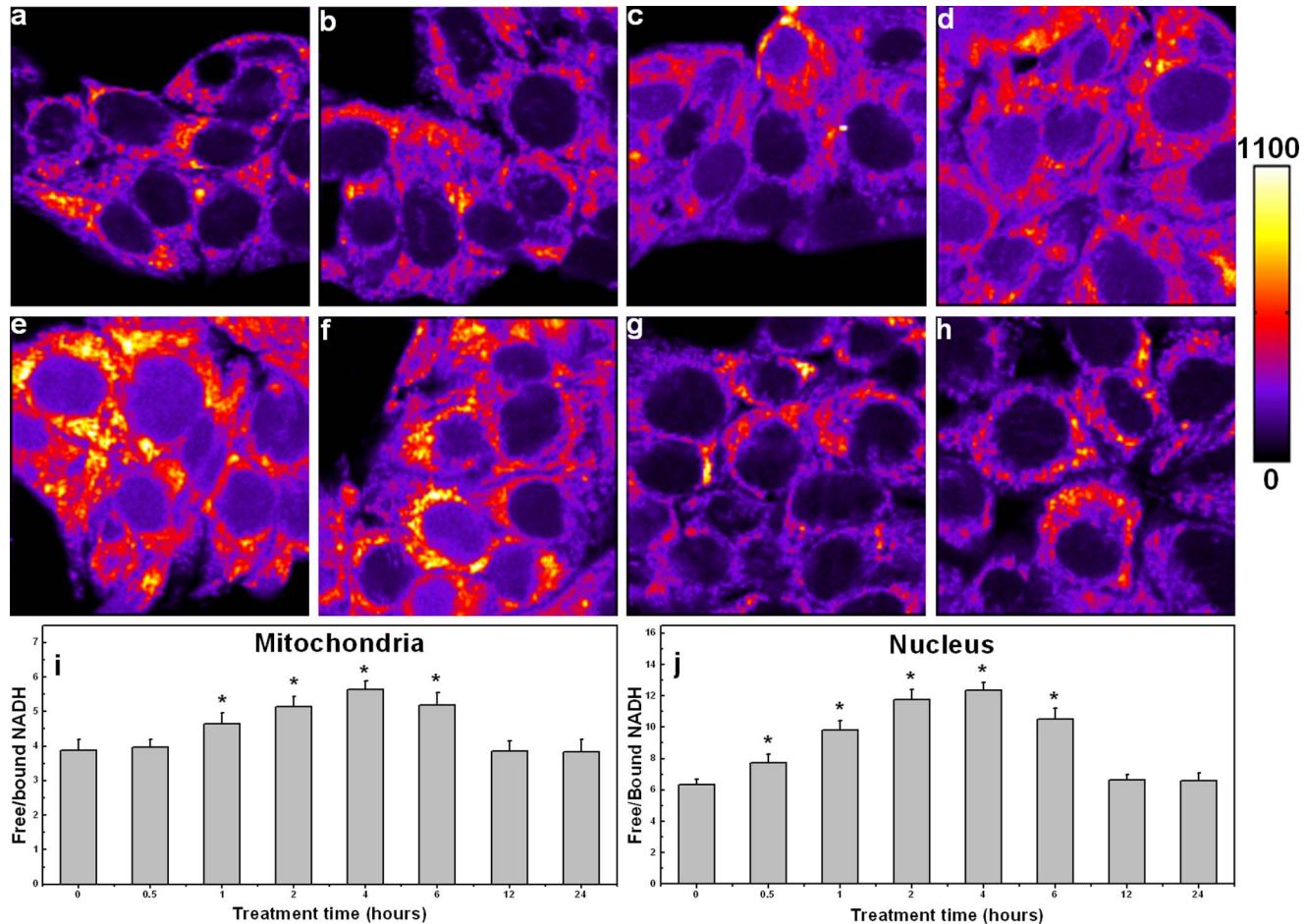


Fig. 2 Response of HepG2 cells after exposure to 5 μM Cd at different time (0, 0.5, 1, 2, 4, 6, 12 and 24 h after exposure to Cd): (a) NADH fluorescence intensity image of the control state, (b) after 0.5 h of treatment, (c) at 1 h, (d) at 2 h, (e) at 4 h, (f) at 6 h, (g) at 12 h, (h) at 24 h, and (i) and (j) changes of free/bound NADH ratio in mitochondria and nucleus at different treatment times. The free/bound NADH ratios were calculated based on averaging the fitting results in the 430 to 470-nm wavelength band; * indicates that the value is significantly different from that in the control state (maximal $p < 0.01$).

ing of the toxic level induced by Cd. A dual-exponential model was used to fit the decay of NADH fluorescence to extract the short-lifetime free NADH and long-lifetime bound NADH signals.^{15,17}

It is known that to achieve stable and accurate fitting of fluorescence decay based on a dual-exponential function, the photon counts at the peak of a fluorescence decay curve should be at least 1000.²³ However, the maximal total counts per pixel in all the images were less than 1000. Therefore, we summed the signals in mitochondrial and nuclear compartments, respectively, to produce high-quality fluorescence decay signals (peak counts > 1000) for the fitting analysis.¹⁷ Representative summed fluorescence decay curves measured from mitochondrial and nuclear compartments are shown in Fig. 3, where blue dots are summed curves measured from a control sample, red lines are fitting curves, green lines are the instrument response function, and black lines are the residuals, respectively. As we can see in Fig. 3, excellent fittings were achieved by using the summed decay curves because χ^2 values were small and close to 1.

To measure the free and protein-bound NADH signals in cells, the cellular fluorescence was analyzed using a dual-

exponential model to extract the decay-associated spectral signals. It was found that at a 730-nm excitation the short- and long-lifetime decay-associated fluorescence spectra were dominated by free and protein-bound NADH signals, respectively. The free/bound NADH ratios of mitochondrial and nuclear compartments in the time course on exposure to 5 μM Cd, the sublethal concentration, are shown in Figs. 2(i) and 2(j). As we can see, the ratio increased in both compartments and reached the peak value at 4 h. In the nuclear compartment, a significant elevation was observed as early as 0.5 h. These results show that the increase of NADH fluorescence intensity observed in Figs. 2(a)–2(h) could be mainly contributed by the elevation of free NADH. More importantly, it was found that the free to protein-bound NADH ratio in both compartments returned to the control level at 12 h, suggesting that cells survived the Cd-induced toxicity to a certain extent. Again, the Wilcoxon test was used to compare the NADH ratio values between of the control and treated groups. In the mitochondrial compartment, the difference in NADH ratio between the treated and control groups was statistically significant (p value < 0.01) over the time course from

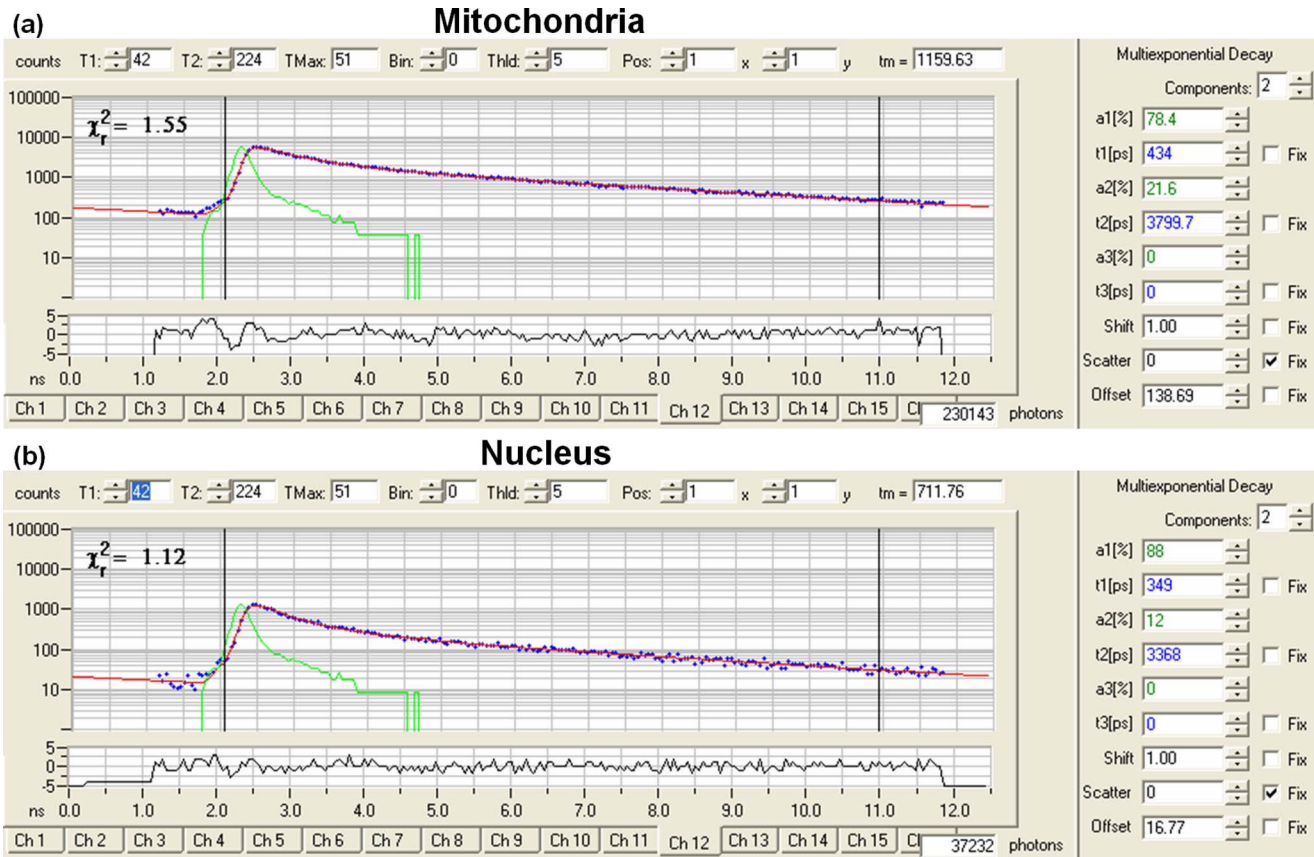


Fig. 3 Representative summed fluorescence decay curves and fitting results of (a) the mitochondrial and (b) the nuclear compartments. (Color online only.)

1 to 6 h after the cell samples exposed to 5 μM Cd. In the nuclear compartment, the NADH ratio measured from the treated groups became significantly different from that of the control groups after half an hour of exposure to Cd. The sta-

tistically significant difference ended at about the same time as that in the mitochondrial compartment.

The Cd-induced increases of the free/bound NADH ratio in mitochondria and nucleus could be explained by the inhibition effect on the electron transfer chain (ETC) and the stimulation effect on the glycolysis pathway, respectively. A

Table 1 Free and protein-bound NADH lifetimes measured from HepG2 cells during the time course of treating with 5 μM Cd.^a

	Mitochondria		Nucleus	
	τ_1 (ns)	τ_2 (ns)	τ_1 (ns)	τ_2 (ns)
Control	0.42 \pm 0.03	3.74 \pm 0.29	0.37 \pm 0.04	3.50 \pm 0.29
0.5 h	0.42 \pm 0.05	3.77 \pm 0.23	0.36 \pm 0.04	3.42 \pm 0.24
1 h	0.40 \pm 0.02	3.68 \pm 0.11	0.36 \pm 0.02	3.43 \pm 0.16
2 h	0.39 \pm 0.04	3.67 \pm 0.18	0.34 \pm 0.04	3.18 \pm 0.12
4 h	0.39 \pm 0.05	3.65 \pm 0.29	0.33 \pm 0.05	3.04 \pm 0.11
6 h	0.40 \pm 0.04	3.65 \pm 0.25	0.35 \pm 0.04	3.16 \pm 0.15
12 h	0.41 \pm 0.03	3.70 \pm 0.15	0.35 \pm 0.03	3.40 \pm 0.13
24 h	0.40 \pm 0.02	3.74 \pm 0.16	0.36 \pm 0.02	3.41 \pm 0.13

^aLifetimes are calculated based on averaging the fitting results in the 430- to 470-nm wavelength band, where the NADH fluorescence peaked.

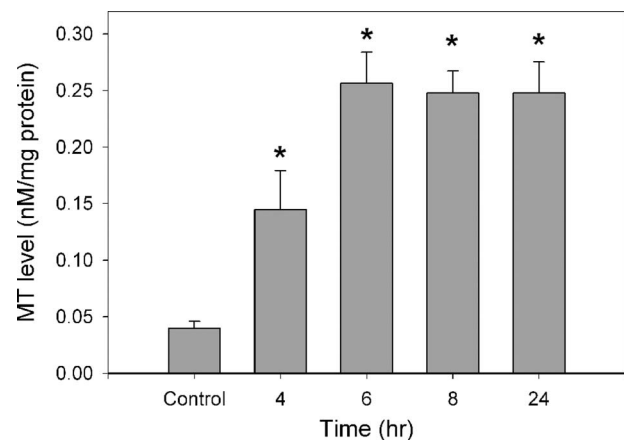


Fig. 4 MT content in HepG2 cells at different times with the treatment by 5 μM Cd. Each value represents the mean and standard deviation of three replications; * indicates that a value is significantly different (maximal $p < 0.01$) from that in the control at 0 h.

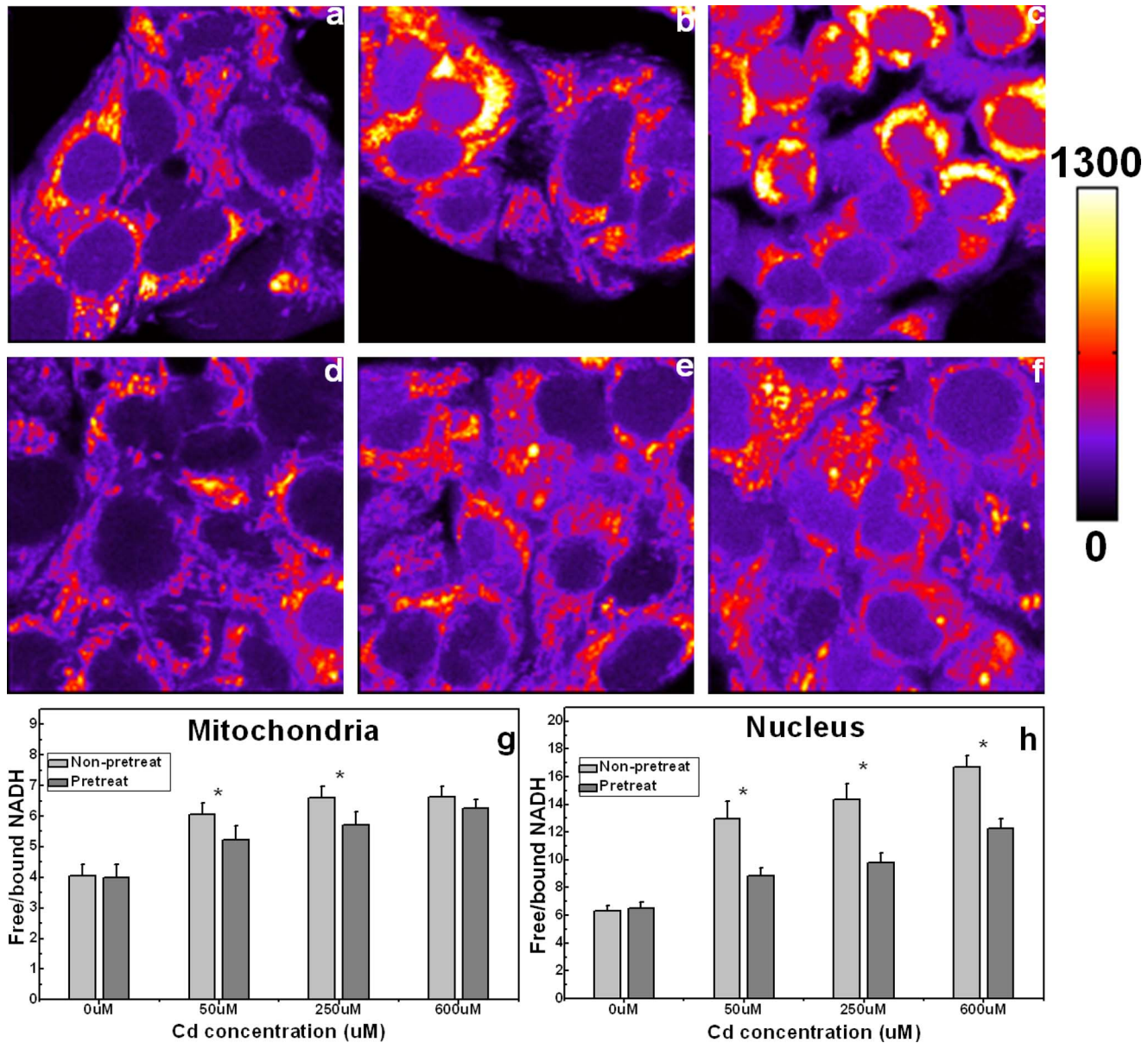


Fig. 5 Responses of HepG2 cells with and without pretreatment with a sublethal concentration of Cd to subsequent exposure to high concentrations of Cd for 2 h: (a) NADH fluorescence intensity image of HepG2 cells without pretreatment after exposure to 50 μM Cd, (b) 250 μM Cd, and (c) 600 μM Cd, and (d) NADH fluorescence intensity image of HepG2 cells with pretreatment after exposure to 50 μM Cd, (e) 250 μM Cd, and (f) 600 μM . (g) and (h) Changes of the free/bound NADH ratio response in the mitochondrial and the nuclear compartments. Free/bound NADH ratios are calculated based on averaging the fitting results in the 430 to 470-nm wavelength band; * indicates that the value is significantly different from that in the control state (maximal $p < 0.02$).

recent study showed that Cd induces a reversible inhibition effect on ETC mainly by binding to the Q_0 site of complex III, which is responsible for the reactive oxygen species (ROS) production in mitochondria.⁵ ROS is an important cellular oxidative stress marker and could induce the ROS-sensitive antioxidant MT protein synthesis. Therefore, the accumulation of free NADH in mitochondria was caused by the ETC inhibition effect of Cd, similar to the inhibition effect induced by NaCN, a well-known ETC inhibitor.^{15,17} Thus, the free/bound NADH ratio could serve as a sensitive indicator for the oxidative stress level in mitochondria when cells are exposed to Cd.

Since there is no NAD^+/NADH conversion mechanism in the nucleus, the increase of free NADH in the nucleus is mostly due to the fact that the NADH produced via certain pathways in cytosol or mitochondria diffuses freely through the nuclear pore.²⁴ However, it is known that the mitochondrial membrane is semipermeable and blocks the diffusion of free NADH from mitochondria to cytosol.²⁵ Therefore, the NADH produced in cytosol should be the source to elevate the free NADH level in the nucleus. Dailianis and Kaloyianni¹¹ revealed that the activity of pyruvate kinase (PK), a key glycolytic enzyme, increases significantly as early

as 30 min after treatment with sublethal concentration of Cd, suggesting that Cd may accelerate the production of free NADH via the glycolysis pathway in cytosol. It is known that Cd could break down the cell-to-cell adhesion by disrupting the E-cadherin protein.¹ Moreover, the Cd-induced free NADH increase in the nucleus would further suppress the expression of E-cadherin by regulating the corepressor protein carboxy-terminal binding proteins^{24,26,27} (CtBP), which is the behavior of a carcinogen.

The free and bound NADH lifetime parameters of mitochondrial and nuclear compartments calculated from the time-lapse measurements of cell culture exposure to 5 μM Cd are summarized in Table 1. As we can see, the short and long lifetimes (τ_1 and τ_2) of NADH fluorescence in the mitochondrial compartment remained relatively constant during the treatment with the sublethal concentration of Cd, whereas, τ_1 and τ_2 of NADH fluorescence decreased in the nuclear compartment and reached a minimum value at 4 h of treatment. Similar to the free/bound NADH ratio tendency, two lifetimes of NADH fluorescence in the nuclear compartment almost returned to the value in the control state at 12 h. Since the protein-bound NADH fluorescence lifetime is particularly sensitive to the change of the NADH binding profile,¹⁶ the Cd-induced changes in the fluorescence lifetimes in the nuclear compartment indicates Cd treatment may interfere with the function of the enzymes to which NADH bind in the nucleus.¹³ The change of short-lifetime NADH (τ_1) shows that although the short-lifetime component of cellular NADH fluorescence decay is dominated by the free-NADH signal, certain interferences from the protein-bound NADH signal remain, which is consistent with previous study.¹⁵

MTs are well-known metal-binding proteins that protect cells against Cd-induced toxicity.⁷ The results in Fig. 4 show that the level of MT protein was significantly elevated in cells at 4 h after exposure to sublethal concentration Cd, because the p value of the MT level at 4 h of treatment versus that at the control point calculated from the Wilcoxon test was less than 0.01. The MT level reached maximum at 6 h, and remained elevated thereafter. This inversely correlates well with the changes of free/bound NADH ratios shown in Fig. 2. Accompanying the significant elevation of MT resulting from a 4-h treatment, the free/bound NADH ratio reached to peak value at 4 h of treatment and then decreased gradually to the value at the control level. To further investigate whether free/bound NADH ratio provides a quantitative indication of MT protection of cells from Cd-induced cytotoxicity, we compared the responses of cell samples with and without pretreatment of a sublethal concentration of Cd to subsequent exposure to much higher Cd doses. Here, the pretreated samples were first exposed to a sublethal concentration of Cd (5 μM) for 24 h. Then two groups of samples were treated with 50, 250, and 600 μM Cd, respectively. The free/bound NADH ratios were measured at 2 h after the exposure to the high concentration of Cd. The NADH fluorescence intensity images recorded from the samples with and without pretreatment are shown in Figs. 5(a)–5(c) and Figs. 5(d)–5(f), respectively. As we can see, after 2 h of exposure to a high concentration of Cd, the cells without the pretreatment of a sublethal concentration of Cd began to detach from coverslip and the cell bodies became round. These are the typical indications of cell

apoptosis.²⁸ In contrast, no obvious morphological change was observed in the cells with the pretreatment of a sublethal concentration of Cd. The free/bound NADH ratios of mitochondrial and nuclear compartments measured from the samples with and without pretreatment are shown in Figs. 5(g) and 5(h). As we can see, because the pretreatment with a sublethal concentration of Cd induced the synthesis of MT proteins, the free/bound NADH ratios of the pretreated cell samples after the exposure to a high concentration Cd were significantly different from those without pretreatment (p value < 0.02) except that in the mitochondrial compartment after 600 μM Cd treatment (p value = 0.18). The results show that MT protein induced by exposure to a sublethal concentration of Cd produces an effective defense against a subsequent high-dose Cd treatment.

4 Conclusion

We demonstrated a noninvasive method based on time-resolved TPEF microscopy for time-lapse sensing of Cd-induced cytotoxicity. When cells were exposed to a sublethal concentration of Cd, the free/bound NADH ratio in the cells extracted from the temporal characteristics of cellular fluorescence was well correlated with the cell viability and MT synthesis, respectively. The correlations suggested that free/bound NADH ratio in cells could be used as a quantitative indicator for the assessment of cytotoxic level. A Cd-induced increase of free/bound NADH ratio in the nucleus is mainly contributed to by from the accelerated glycolysis process, while the Cd-induced inhibition effect on the electron transfer chain is responsible for the elevation of the free/bound NADH ratio in mitochondria. Our experimental results show that the elevation of free/bound NADH ratio caused by subsequent exposure to a high concentration of Cd could be significantly suppressed by pretreatment with a sublethal concentration of Cd. This important evidence demonstrates that the induction of MT protein in the exposure to a sublethal concentration of Cd provides cells a natural defense mechanism against Cd toxicity.

Acknowledgments

This work is supported by the Hong Kong Research Grants Council through Grants No. HKUST6408/05M and No. HKUST618808.

References

1. C. A. Pearson and W. C. Prozialeck, "E-Cadherin, β -Catenin and cadmium carcinogenesis," *Med. Hypotheses* **56**, 573–581 (2001).
2. B. A. Fowler, "General subcellular effects of lead, mercury, cadmium, and arsenic," *Environ. Health Perspect.* **22**, 37–41 (1978).
3. T. C. Hutchinson and K. M. Meema, *Lead, Mercury, Cadmium, and Arsenic in the Environment*, John Wiley & Sons, New York (1987).
4. R. Wittman and H. Hu, "Cadmium exposure and Nephropathy in a 28-year-old female metals worker," *Environ. Health Perspect.* **110**, 1261–1266 (2002).
5. Y. Wang, J. Fang, S. S. Leonard, and K. M. K. Rao, "Cadmium inhibits the electron transfer chain and induces reactive oxygen species," *Free Radic Biol. Med.* **36**, 1434–1443 (2004).
6. M. K. Choi, B. H. Kim, Y. Y. Chung, and M. S. Han, "Cadmium-induced apoptosis in h9c2, a7r5, and c6-gliial cell," *Bull. Environ. Contam. Toxicol.* **69**, 335–341 (2002).
7. C. D. Klaassen, J. Liu, and S. Choudhuri, "Metallothionein: an intracellular protein to protect against cadmium toxicity," *Annu. Rev. Pharmacol. Toxicol.* **39**, 267–294 (1999).

8. U. Wimmer, Y. Wang, O. Georgiev, and W. Schaffner, "Two major branches of anti-cadmium defense in the mouse: MTF-1/metallothioneins and glutathione," *Nucleic Acids Res.* **33**, 5715–5727 (2005).
9. P. M. Hinkle and M. E. Osborne, "Cadmium toxicity in rat pheochromocytoma cells: studies on the mechanism of uptake," *Toxicol. Appl. Pharmacol.* **124**, 91–98 (1994).
10. M. S. Yang, K. P. Lai, K. Y. Cheng, and C. K. Wong, "Changes in endogenous Zn and Cu distribution in different cytosolic protein fractions in mouse liver after administration of a single sublethal dose of CdCl₂," *Toxicology* **154**, 103–111 (2000).
11. S. Dailianis and M. Kaloyianni, "Cadmium induces both pyruvate kinase and Na⁺/H⁺ exchanger activity through protein kinase C mediated signal transduction, in isolated digestive gland cells of *Mytilus galloprovincialis* (L.)," *J. Exp. Biol.* **207**, 1665–1674 (2004).
12. M. K. Campbell, *Biochemistry*, Saunders College Publishing, Orlando, FL (1995).
13. B. Tandogan and N. N. Ulusu, "The inhibition kinetics of yeast glutathione reductase by some metal ions," *J. Enzyme Inhib. Med. Chem.* **22**, 489–495 (2007).
14. D. K. Bird, L. Yan, K. M. Vrotsos, K. W. Eliceiri, E. M. Vaughan, P. J. Keely, J. G. White, and N. Ramanujam, "Metabolic mapping of MCF10A human breast cells via multiphoton fluorescence lifetime imaging of the coenzyme NADH," *Cancer Res.* **65**, 8766–8773 (2005).
15. Y. Wu, W. Zheng, and J. Y. Qu, "Sensing cell metabolism by time-resolved autofluorescence," *Opt. Lett.* **31**, 3122–3124 (2006).
16. M. C. Skala, K. M. Riching, D. K. Bird, A. G. Fitzpatrick, J. Eickhoff, K. W. Eliceiri, P. J. Keely, and N. Ramanujam, "In vivo multiphoton fluorescence lifetime imaging of protein-bound and free nicotinamide adenine dinucleotide in normal and precancerous epithelia," *J. Biomed. Opt.* **12**, 024014 (2007).
17. D. Li, W. Zheng, and J. Y. Qu, "Time-resolved spectroscopic imaging reveals the fundamentals of cellular NADH fluorescence," *Opt. Lett.* **33**, 2365–2367 (2008).
18. T. Lin and M. S. Yang, "Benzo[a]pyrene-induced elevation of GSH level protects against oxidative stress and enhances xenobiotic detoxification in human HepG2 cells," *Toxicology* **235**, 1–10 (2007).
19. D. L. Eaton and B. F. Toal, "Evaluation of the Cd/hemoglobin affinity assay for the rapid determination of metallothionein in biological tissues," *Toxicol. Appl. Pharmacol.* **66**, 134–142 (1982).
20. M. S. Yang, D. Li, T. Lin, J. J. Zheng, W. Zheng, and J. Y. Qu, "Increase in intracellular free/bound NAD[P]H as a cause of Cd-induced oxidative stress in the HepG2 cells," *Toxicology* **247**, 6–10 (2008).
21. W. Zheng, Y. Wu, D. Li, and J. Y. Qu, "Epithelial autofluorescence: single- versus two-photon excitation," *J. Biomed. Opt.* **13**, 054010 (2008).
22. A. Mayevsky and B. Chance, "Oxidation-reduction states of NADH *in vivo*: From animals to clinical use," *Mitochondrion* **7**, 330–339 (2007).
23. *Manual of SPCImage 2.8 Data Analysis Software for Fluorescence Lifetime Imaging Microscopy*, Becker & Hickl GmbH, Berlin, Germany (2005).
24. C. C. Fjeld, W. T. Birdsong, and R. H. Goodman, "Differential binding of NAD⁺ and NADH allows the transcriptional corepressor carboxyl-terminal binding protein to serve as a metabolic sensor," *Proc. Natl. Acad. Sci. U.S.A.* **100**, 9202–9207 (2003).
25. W. Ying, "NAD⁺/NADH and NADP⁺/NADPH in cellular functions and cell death: regulation and biological consequences," *Antioxid. Redox. Sign.* **10**, 1–28 (2008).
26. Q. Zhang, S. Y. Wang, A. C. Nottke, J. V. Rocheleau, D. W. Piston, and R. H. Goodman, "Redox sensor CtBP mediates hypoxia-induced tumor cell migration," *Proc. Natl. Acad. Sci. U.S.A.* **103**, 9029–9033 (2006).
27. Q. Zhang, D. W. Piston, and R. H. Goodman, "Regulation of corepressor function by nuclear NADH," *Science* **295**, 1895–1897 (2002).
28. G. Hacker, "The morphology of apoptosis," *Cell Tissue Res.* **301**, 5–17 (2000).